'94 KACC (1994. 10. 17 ~ 20)

A Unifying Design of H_∞ Controller with PI Speed Feedback for High Precision Position Control of Flexible System

Yeonghan Chun & Yoichi Hori

Department of Electrical Engineering
The University of Tokyo
7-3-1 Hongo, Bunkyo, Tokyo 113, Japan

Abstract – We propose a design method that uses H_∞ optimization method to suppress oscillation of a shaft between motor and load for high precision(0.001 % of reference input) position control. PI speed control loop was introduced as a minor loop. *Standard problem* is used for the modeling of the system and Glover-Doyle's algorithm is used for the optimization in the H_∞ space. Friction is considered to be an important factor that makes it difficult for the system to reach steady state in short time. In this paper, we propose a hybrid controller that includes PI speed feedback loop, which is expected to have a role to reject torque disturbance like friction.

1. Introduction

For the high precision position control, oscillation of shaft becomes an important factor even though its stiffness constant is big enough. And, friction works as torque disturbance nonlinearly, which makes it difficult for the system to reach steady state in short time. In industry, these problems are big obstacle to enhance productivity. In a certain application, the requirements of controller are very severe for the productivity, for example, step response should reach steady state in 0.4 seconds together with the suppression of oscillation of a shaft between motor and load. Generally PI or P controller has been used to get these requirements, but it showed some limitations that oscillation has high frequency components while required step response is obtained. Several papers[9, 10] reported improved performances against this kind of problems. The authors[11] also applied H_∞ optimization method to the speed control of steel rolling mill, which can be modelled by two mass system.

Since H_∞ theory was introduced by Zames, the H_∞ theory has been developed by many researchers. Now, software program is available for the *standard problem*. Thus, the *standard problem* is used for the modeling of the system , and Glover-Doyle algorithm was used for the H_∞ optimization in this paper. As PI speed feedback loop has a role to reject disturbance, it is expected to enhance the performance of position controller. So we introduced PI speed feedback loop as a minor loop, and it could be shown that the PI speed feedback loop with high gain helped reduce settling time compared with the case with H_∞ controller only. All results will be confirmed by the computer simulation.

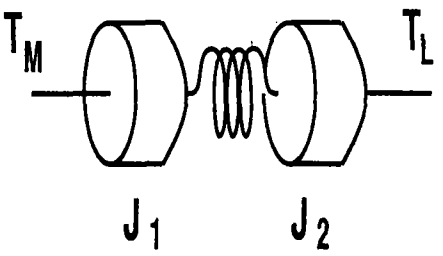

Figure 1: Two mass system for position control

2. System Description and Modeling

The flexible system for the position control can be explained by Figure 1. Motor is connected to a load through a shaft with a certain stiffness constant. This coulpled system can be modelled by two mass system as in Figure 2, which is the simplest model of the flexible system. Feedback signal of speed is measured at the motor side, and the PI speed controller C_v works against the disturbance like load change and friction. And high gain of this PI speed controller helps the system to reach steady state in short time. As high gain of speed controller causes a high frequency oscillation of shaft, we have to be careful to choose the gain appropriately.
Transfer function of PI speed feedback controller is given by equation 1.

$$C_v = \frac{K_v(T_v s + 1)}{T_v s} \tag{1}$$

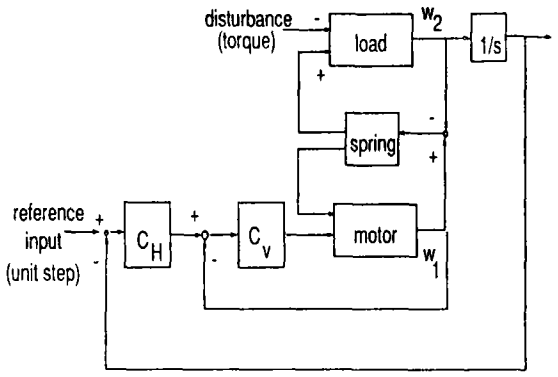

Figure 2: Block diagram of the two mass system with PI speed controller C_v and H_∞ position controller C_H

where,

$$K_v = 7 \times 10^3$$
$$T_v = 0.002 \text{ sec}$$

And, other transfer functions and parameters are given by equation $2 \sim 4$.

$$\text{motor}: \quad \frac{1}{J_M s} \tag{2}$$

$$\text{spring}: \quad \frac{K}{s} + D \tag{3}$$

$$\text{load}: \quad \frac{1}{J_L s} \tag{4}$$

where,

$$J_M = 5\ Kgm^2$$
$$J_L = 5\ Kgm^2$$
$$K = 10^5\ N/m$$
$$D = 1000\ N/m/s$$

As we can notice from Figure 2, motor speed is fed back to the speed controller, but we want to track the load position. This PI speed controller has an effect to guide position as the controller has integrator term. High gain of the conventional PI controller makes the response to be oscillatory with high frequency components, but practically it is expected to help the system to reach steady state in short time against nonlinear friction.

Position of load side is measured by laser interferometer for the measurement of high precision position and it is fed back to the position controller. The noise propagation characteristics of laser interferometer can be explained by the complementary sensitivity function. When the modeling uncertainty is positioned at the load output as a multiplicative perturbation, the robust stability condition can be explained by this complementary sensitivity function too.

Figure 3 shows the augmented system with weighting functions which shape the input singals. The conventional PI position controller has been substituted by H_∞ controller C_H.

3. Mathematical Modeling for Optimization

Standard problem for H_∞ optimization can be explained by transfer functions in the frequency domain.
Let

$$\Delta = 1 + C_V T_M + T_S T_L + T_M T_S + C_V T_M T_S T_L + C_H C_V T_M T_S T_L \frac{1}{s} \tag{5}$$

then,

$$\frac{x_2}{r} = \frac{C_H C_V T_M T_S T_L}{s\Delta} \tag{6}$$

$$\frac{e_1}{r} = \frac{1 + C_V T_M + T_S T_L + T_M T_S + C_V T_M T_S T_L}{\Delta} \tag{7}$$

$$\frac{e_2}{r} = \frac{C_H C_V T_M (1 - T_S T_L)}{s\Delta} \tag{8}$$

$$\frac{e_1}{d} = \frac{T_L(1 + C_V T_M + T_M T_S)}{s\Delta} \tag{9}$$

$$\frac{e_2}{d} = \frac{-T_L C_H C_V T_M \frac{1}{s} - T_L(1 + T_M TS + C_V T_M)}{s\Delta} \tag{10}$$

$$\frac{e_1}{p} = \frac{-(1 + T_S TL)}{s\Delta} \tag{11}$$

$$\frac{e_2}{p} = \frac{e_1}{r} \tag{12}$$

$$\frac{y}{p} = -\frac{x_2}{r} = R_T \tag{13}$$

Two port diagram for the modeling of standard problem is given by Figure 4, which is equivalent to Figure 3.

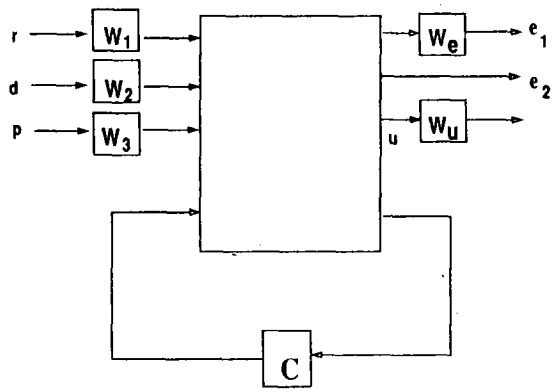

Figure 4: Two port block diagram equivalent to Figure 3

As we can see from Figure 4, the robust stability condition is not used as a criterion in the synthesis procedure. This is why structured perturbation should be introduced and thus D-K iteration should be done for the optimization. As current D-K iteration does not guarantee the existence of solution and results in the increase of order of controller, we avoid to use D-K iteration. Therefore we did not use robust stability criterion while we synthesize the controller, but checked if the controller satisfy the robust stability condition after designing the controller. As a result, the cost function of the optimization in the H_∞ space is given by equation 14.

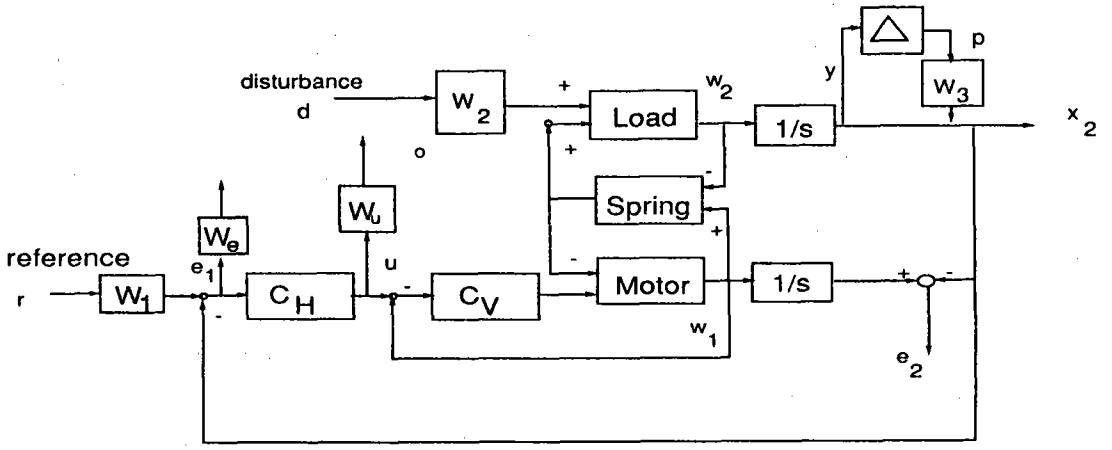

Figure 3: Block diagram of the augmented system

$$\min_{stabilizing C} \left\| \begin{matrix} W_1 S_{e_1 r} & W_2 S_{e_1 d} & W_3 S_{e_1 p} \\ W_1 S_{e_2 r} & W_2 S_{e_2 d} & W_3 S_{e_2 p} \\ W_1 W_u \frac{u}{r} & W_2 W u \frac{u}{d} & W_3 W_u \frac{u}{p} \end{matrix} \right\|_\infty = \gamma \quad (14)$$

4. Robust Stability Condition and Noise Propagation

From the small gain theorem, robust stability condition is given by equation 13 and 15.

$$\|R_T\|_\infty < 1 \quad (15)$$

So, gain of R_T should be less than one over the frequency range. And, we can see that the transfer function R_T also decides the noise propagation characteristics, too. Therefore, the robust stability condition can be satisfied by shaping the complementary sensitivity function, and thus noise propagation characteristics can be determined by this complementary sensitivity function.
Figure 5 shows the gain characteristics of complementary sensitivity function with designed controller.

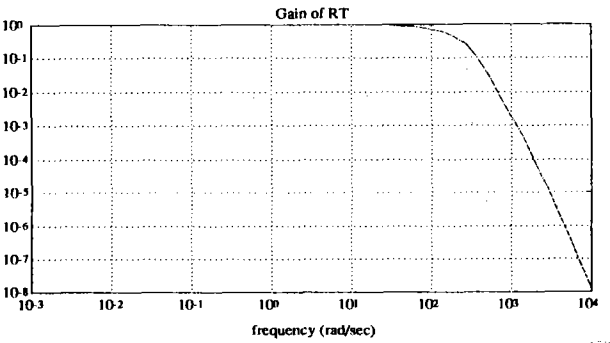

Figure 5: Bode diagram of R_T

5. Weighting Functions

Weighting functions are decided to shape the signals. This is one way of deciding weighting functions. For example, weighting functions W_1, W_2 and W_3 are decided to represent frequency characteristics of each input signal. As W_1 is weighting function for command reference of step function, it was given by equation 16, which is the approximation of $1/s$, since every weighting function should be element of the H_∞ space.

Weighting function W_2 is decided to be equation 17. This weighting function is to shape the signal to represent high frequency components, that is caused by the modeling uncertainty. Generally, modeling uncertainty like time delay appears significantly at high frequency. But, the gain of each weighting function has a role of putting weight between the weighting functions, thus we can see the trade off relationships between each weighting function.

Weighting function W_3 is given by equation 18, which is based on the assumption that torque disturbance has low frequency components. Actually this assumption can be controversial since torque disturbance due to nonlinear coulomb friction is not so simple to be explained by frequency characteristics.

One of the important weighting functions is W_u, which is used to shape control effort. Designed controller without considering weighting function W_u sometimes give high frequency signals as control, which represents that the controller itself generates noise terms. In this case, we can avoid high frequency control effort by putting high frequency weighting function at W_u, this is very important in practice.

Weighting functions W_e has a role to give a weight to the tracking error of cost function among other output signals e_2 and u.

Weighting functions used for designing position con-

troller are summarized by equation 16 $\sim$ 20.

$$W_1 = \frac{0.001s+1}{s+0.001} \quad (16)$$

$$W_2 = \frac{100(s+100)}{s+100000} \quad (17)$$

$$W_3 = \frac{0.001s+1}{s+0.001} \quad (18)$$

$$W_u = \frac{10(s+10)}{s+100000} \quad (19)$$

$$W_e = 10 \quad (20)$$

6. Simulation Results

In order to avoid satuarting the amplifier, the desired trajectory must be chosen carefully. The trajectory used for the simulation is given by equation 22, which is smooth.

$$0.5 * sin(\frac{2\pi}{0.1} - \frac{\pi}{2}) \quad (t < 0.05) \quad (21)$$
$$1 \quad (t \geq 0.05)$$

This trajectory corresesponds to 1.0 rad displacement and 50 msec of transition time. The corresponding figure is ginven by Figure 6.

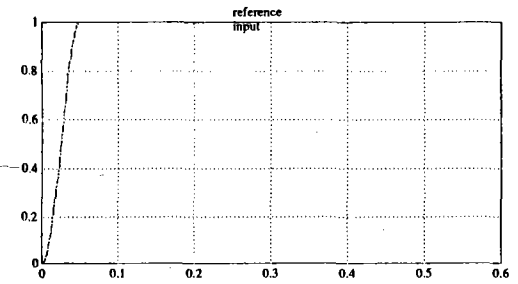

Figure 6: Reference input

The conventional position controller is given by equation 22 , which has been used practically.

$$C_p = \frac{K_p}{T_p s + 1} \quad (22)$$

Gain of the conventional controller which has the transfer function of equation 22 was decided to have the same gain of H_∞ controller at low frequency, in which case each parameters of C_p are given by $K_p = 56.3$ and $T_p = 0.0046$.

Bode plots of two controllers, the conventional controller C_p and H_∞ controller, are given by Figure 7.

Simulation results with unifying method is compared with those of conventional position controller. 20 % of parameter variations were modelled to see the robustness of designed controller, and 10 Nm of torque disturbance were added to the load at 0.4 second.

Each figure of the simulation results shows output response, tracking error and control input respectively downards. Figure 8 and Figure 9 represent the simulation result when nominal data were used. Two figures show almost the same characteristics.

20 % of parameter variations at load inertia J_l and stiffness constant K_{12} was considered to see the robustness of the designed controller. The most severe case is when inertia J_l was underestimated, and stiffness constant K_{12} was overestimated, as Figure 11 shows. From Figure 9 and 11, we can see that H_∞ controller is robuster than conventional position controller.

References

[1] Balas, G.J.(1991) and J.C. Doyle and K. Glover,A. Packard and R. Smith, μ-Analysys and Synthesis Toolbox : User's Guide, MuSyn Inc., Minneapolis MN, USA

[2] Chiang, R.Y. and M.G. Safonov(1992), Real K_m-synthesis via generalized Popov multipliers, ACC/TP9, 2417-2418

[3] Doyle, J.C. and K. Glover and P. Khargonekar and B. Francis(1989), State-space solutions to standard H_2 and H_∞ problems, IEEE Transactions on Automatic Control, vol. 34, no. 8

[4] Francis, B.A.(1987), Lecture Notes in Control and Information Sciences : A Course in H_∞ Control Theory, Springer-Verlag, New York, USA

[5] Hori, Y.(1992), Comparison of Vibration Suppression Control Strategies in 2-mass system Including a Novel Two-Degree-of-Freedom H_∞ Ccontroller, IEEE 2nd AMC Workshop, 409-416

[6] Hori, Y.(1994), 2-Mass System Control Based on Resonance Ratio Control and Manabe Polynomials, the Fivrst Asian Control Conference, SP-16-2

[7] Iseki, H. and Y. Hori(1994) Advanced Controller for Two-mass System Using Loop Shaping Design Techniques , 3rd International Workshop on Advanced Motion Control, Berkeley

[8] Matsui, N and Y. Hori(1993), New Technologies on Motor Control, Trans. of IEE-Japan, Vol.113-D, No.10,1122-1137

[9] Lee, Ho S and M. Tomizuka(1994), Robust High-Speed Servo-Controllers for Micropositioning Systems, IEEE AMC Workshop, 633-642

[10] Sato, M and S. Wakui and S. Hara(1994), An H_∞ Control for Positioning of XY Stage Based on a Loop Shaping Procedure, ASCC, Vol. 2, 625-628

[11] Chun, Y.H and Y. Hori(1994), Rolling Mill Controller Design with H_∞ Sensitivity Minimization, ASCC, vol. 2, 629-632

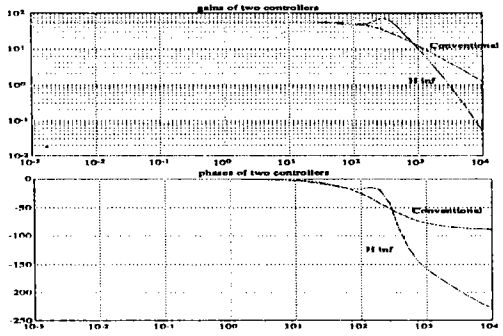

Figure 7: Bode plot of the conventional controller C_p and H_∞ Controller

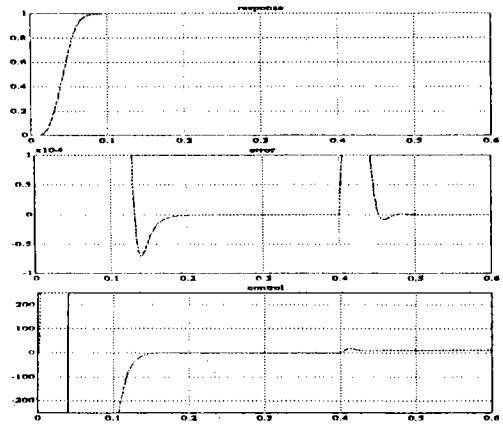

Figure 8: Response, tracking error, and control input when nominal data were used with H_∞ Controller

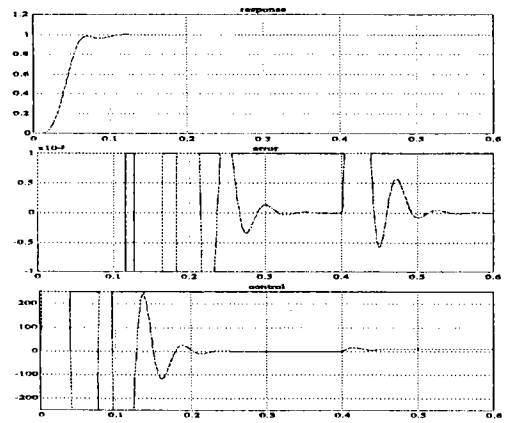

Figure 9: Response, tracking error, and control input when nominal data were used with convertional controller C_p

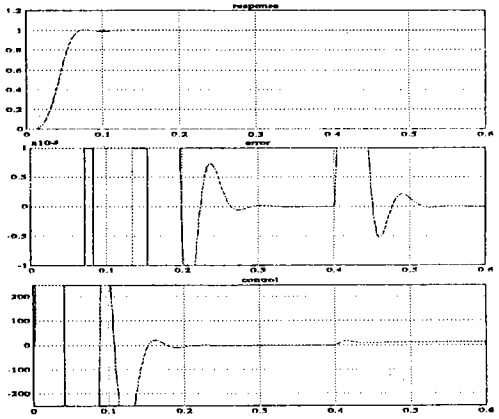

Figure 10: Response, tracking error, and control input when 20 % of parameter variations were modelled with H_∞ controller, $K_{12} \rightarrow K_{12} \times 0.8$ and $J_l \rightarrow J_l \times 1.2$

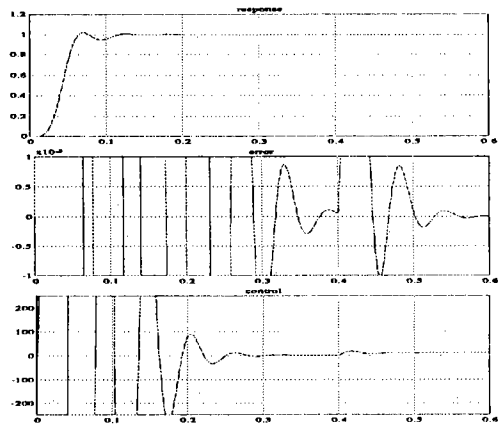

Figure 11: Response, tracking error, and control input when 20 % of parameter variations were modelled with conventional controller C_p, $K_{12} \rightarrow K_{12} \times 0.8$ and $J_l \rightarrow J_l \times 1.2$